Theory of surface spin waves in a stacked triangular antiferromagnet with ferromagnetic interlayer coupling

E. Meloche,[1,*] C. M. Pinciuc,[2] and M. L. Plumer[1]
[1]*Department of Physics and Physical Oceanography, Memorial University of Newfoundland, St John's, Newfoundland, Canada A1B 3X7*
[2]*Edward S. Rogers Sr. Department of Electrical and Computer Engineering, University of Toronto, Ontario, Canada M5S 3G4*
(Received 9 May 2006; revised manuscript received 11 July 2006; published 21 September 2006)

A theory is presented for bulk and surface spin waves in a stacked triangular antiferromagnet with ferromagnetic interlayer coupling. The method exploits triangular symmetry of the system through properties of block-tridiagonal matrices. A theory is developed for spin-wave dispersion relations of a semi-infinite frustrated system as well as for thin films. The influence of surface exchange and anisotropy parameters on surface and bulk spin-wave energies is discussed. The method is applied to obtain numerical results for $RbFeCl_3$ and $CsCuCl_3$.

DOI: 10.1103/PhysRevB.74.094424 PACS number(s): 75.30.Ds, 75.70.−i

I. INTRODUCTION

Currently there is considerable interest, both theoretical and experimental, on the influence of surfaces on the static and dynamic properties of magnetic materials in reduced dimensions. The magnetic properties of atoms located at surfaces or interfaces can be considerably different from those of atoms within the bulk of the material and interesting new physical phenomena can emerge.[1,2] Understanding the surface properties of magnetic materials is essential for the development of higher density magnetic storage devices and magnetic sensors that are based on multilayer thin film technology. Numerous experimental techniques including inelastic light scattering and spin-wave resonance have been employed for many years to investigate the properties of long-wavelength spin waves near surfaces.[3,4] More recently, spin-wave dispersion in ultrathin ferromagnetic films has been measured up to the edge of the surface Brillouin zone using spin-polarized electron energy loss spectroscopy (SPEELS).[5,6] The theory of surface spin waves in semi-infinite ferromagnets and antiferromagnets (with a single surface) has been investigated by several authors.[7–11] Theoretical techniques developed for semi-infinite systems have been generalized to investigate the spin dynamics in magnetic thin films.[12,13] The effects of magnetically frustrated surfaces on thin films have recently been investigated using Monte Carlo simulations and Green function techniques.[14] The properties of magnetic excitations at the surface of a geometrically frustrated lattice are investigated here using a spin operator formalism.

Magnetically frustrated spin systems are typically characterized with a highly degenerate ground state and are known to exhibit novel physical phenomena.[15,16] In the present work the effect of surfaces on the excitation spectrum of a stacked triangular antiferromagnet with easy-plane anisotropy is examined. The spin-wave dispersion relation is obtained for a semi-infinite system and the calculations are generalized to investigate the excitation spectra in finite-thickness lattices. Geometrical frustration within any particular layer is due to the triangular arrangement of antiferromagnetically coupled spins and results in a three-sublattice 120° magnetic order. Simple hexagonal stacking of layers results in no interlayer frustration. In the present work we consider ferromagnetic interaction between the interlayer spins. The technique may be readily extended to the antiferromagnetic case and to frustrated systems with easy-axis anisotropy. Some comments concerning the extension of the model to other magnetically frustrated spin systems are given later.

Linearized spin-wave theory was applied to a 2D triangular antiferromagnet with easy-plane anisotropy using a boson representation for the spin operators.[17] A recent application of the 2D model has been successful for analyzing the spin dynamics in the hexagonal magnetoelectic compound $HoMnO_3$.[18] Neutron scattering techniques have been employed to investigate the magnetic order and properties of bulk excitations in many frustrated systems.[19,20] The bulk spin wave dispersion relation has been calculated using a wide variety of theoretical techniques.[21–24] Surface modes in a frustrated system are inherently different than the previously studied cases because the surface will contain spins belonging to all *three* sublattices, whereas in ferromagnets (or simple cubic antiferromagnets) the surface contains spins belonging to only one (two) sublattice. In this study, surface and bulk dispersion relations are deduced using an operator equation of motion formalism. The equations of motion for the spin operators at each crystal site are formulated and the system of coupled equations is expressed in matrix form. Spin-wave modes are obtained by solving a determinantal condition. The approach used here extends the matrix inversion technique employed earlier for spin waves in two-sublattice antiferromagnetics.[11,13,25]

In Sec. II the microscopic Hamiltonian is described and the spin-wave dispersion relation for an infinite stacked triangular antiferromagnet is derived. In Sec. III the surface and bulk spin-wave spectra are obtained for a semi-infinite system, and in Sec. IV the approach is generalized to investigate excitations in frustrated thin films. Section V contains further discussions and the conclusions of our work.

II. HAMILTONIAN

The hexagonal lattice is characterized by the following spin Hamiltonian:

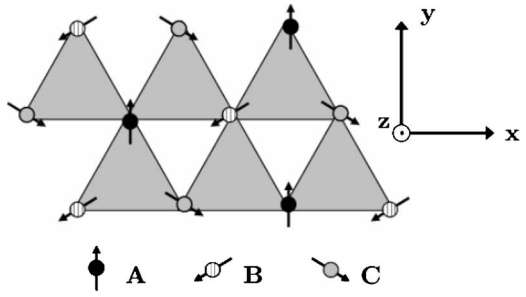

FIG. 1. Planar view of the 120° Néel structure in a frustrated antiferromagnetic. The dark, striped, and shaded spins refer to sites on sublattices A, B, and C, respectively. The global coordinate system is also shown, where the z axis corresponds to the hexagonal c axis.

$$\mathcal{H} = \sum_{\langle i,j \rangle} J_{i,j}(\boldsymbol{S}_i \cdot \boldsymbol{S}_j + \sigma S_i^z S_j^z) - \sum_{\langle i,i' \rangle} J'_{i,i'}(\boldsymbol{S}_i \cdot \boldsymbol{S}_{i'} + \sigma' S_i^z S_{i'}^z) + \sum_i D_i (S_i^z)^2, \tag{1}$$

where $J_{i,j} > 0$ represents the intralayer antiferromagnetic exchange between sites on different sublattices while $J'_{i,i'} > 0$ represents the ferromagnetic interlayer coupling between sites on the same sublattice. Here, nearest-neighbor couplings only are included. The effect of anisotropic exchange is accounted for through the parameters σ and σ'. The parameter D_i describes the strength of the single-ion anisotropy, and here it is assumed that $D_i \geqslant 0$ so that the spins lie in the planes perpendicular to the c axis. The 120° spin configuration of the classical ground state of this model is depicted schematically in Fig. 1.

Following the approach used in previous studies, the lattice is divided into three sublattices A, B, and C, and sites on each sublattice are denoted with indices l, m, and n, respectively. Next, the Hamiltonian (1) is transformed to a local coordinate system such that the new z axis for each sublattice is in the direction of the spin alignment shown in Fig. 1. The transformation for sites on the different sublattices may be written as

$$(S_l^x, S_l^y, S_l^z) \rightarrow (S_l^{x'}, S_l^{z'}, -S_l^{y'}),$$

$$(S_m^x, S_m^y, S_m^z) \rightarrow (S_m^{x'} \cos\theta - S_m^{z'} \sin\theta, S_m^{x'} \sin\theta + S_m^{z'} \cos\theta, -S_m^{y'}),$$

$$(S_n^x, S_n^y, S_n^z) \rightarrow (S_n^{x'} \cos\theta + S_n^{z'} \sin\theta, -S_n^{x'} \sin\theta + S_n^{z'} \cos\theta, -S_n^{y'}), \tag{2}$$

with $\theta = 2\pi/3$. The bulk spin-wave dispersion relation may be obtained by forming the equation of motion for the operators $S_i^{\pm}$ using

$$i\frac{dS_i^{\pm}}{dt} = [S_i^{\pm}, \mathcal{H}] \text{ with } i = l,m,n, \tag{3}$$

where $S_i^{\pm}$ represent local spin deviation operators for sites on each sublattice defined as $S_i^{\pm} = S_i^{x'} \pm iS_i^{y'}$ and H is the transformed Hamiltonian. The exchange terms on the right-hand side (rhs) of Eq. (3) involve the product of operators at different sites which are decoupled using the random-phase approximation (RPA). In the low-temperature limit ($T \ll T_N$) we assume $\langle S_i^{z'} \rangle = S$, where S is the spin quantum number. The terms arising from the single-ion anisotropy involve the product of operators at the same site and are decoupled using $(S_i^{\pm} S_i^{z'} + S_i^{z'} S_i^{\pm}) \rightarrow 2SpS_i^{\pm}$ where $p = [1 - (2S)^{-1}]$.

The resulting homogeneous set of equations are transformed to a wave-vector representation and expressed in matrix form as $\mathbf{Ab} = 0$, where $\mathbf{A}$ is a block-circulant matrix that may be written as

$$\boldsymbol{A} = \begin{pmatrix} \tilde{A} & \tilde{B} & \tilde{B}^* \\ \tilde{B}^* & \tilde{A} & \tilde{B} \\ \tilde{B} & \tilde{B}^* & \tilde{A} \end{pmatrix} \tag{4}$$

and $\mathbf{b} = [S_A^+(\mathbf{k}), S_A^-(-\mathbf{k}), S_B^+(\mathbf{k}), S_B^-(-\mathbf{k}), S_C^+(\mathbf{k}), S_C^-(-\mathbf{k})]^T$. The elements $S_A^+(\mathbf{k})$ and $S_A^-(-\mathbf{k})$ denote the Fourier amplitudes of the spin operators S_l^+ and S_l^-, respectively. The 2×2 matrices $\tilde{A}$ and $\tilde{B}$ in Eq. (4) are defined as

$$\tilde{A} = \begin{pmatrix} E + \Omega & \alpha \\ -\alpha & E - \Omega \end{pmatrix} \text{ and } \tilde{B} = \begin{pmatrix} \beta & \gamma \\ -\gamma & -\beta \end{pmatrix} \tag{5}$$

where

$$\Omega = 2S\cos\theta J(0) - pSD - SJ'(0) + S(2+\sigma')J'(k_z)/2,$$

$$\alpha = pSD - S\sigma' J'(k_z)/2,$$

$$\beta = -S(1/2+\sigma)J(\mathbf{k}_{\|})/2,$$

$$\gamma = S(3/2+\sigma)J(\mathbf{k}_{\|})/2. \tag{6}$$

The exchange integrals $J(\mathbf{k}_{\|})$ and $J'(k_z)$ are defined as

$$J(\mathbf{k}_{\|}) = J(2\cos(k_y\sqrt{3}a/2)\exp(-ik_x a/2) + \exp(ik_x a)),$$

$$J'(k_z) = 2J'\cos(k_z c), \tag{7}$$

with a and c denoting the lattice constants. In writing Eqs. (4) and (5) we have assumed the usual time dependence $\exp(-iEt)$, where E is the mode energy. Bulk spin-wave modes correspond to solutions of the determinantal condition $\det \mathbf{A} = 0$. The matrix $\mathbf{A}$ can be block diagonalized using the unitary transformation $\mathbf{A} = \mathbf{UDU}^{\dagger}$ where

$$\mathbf{D}=\begin{pmatrix}\tilde{\Lambda}(0) & 0 & 0\\ 0 & \tilde{\Lambda}(\theta) & 0\\ 0 & 0 & \tilde{\Lambda}(-\theta)\end{pmatrix},\quad \mathbf{U}=\frac{1}{\sqrt{3}}\begin{pmatrix}\mathbb{1} & \mathbb{1} & \mathbb{1}\\ \mathbb{1} & \exp(i\theta)\mathbb{1} & \exp(-i\theta)\mathbb{1}\\ \mathbb{1} & \exp(-i\theta)\mathbb{1} & \exp(i\theta)\mathbb{1}\end{pmatrix}, \tag{8}$$

and $\mathbb{1}$ is a 2×2 unit matrix. The elements of $\mathbf{D}$ are defined as $\tilde{\Lambda}(\phi)=\tilde{A}+\tilde{B}\exp(i\phi)+\tilde{B}^{*}\exp(-i\phi)$ (for $\phi=0,\pm\theta$) and the spin-wave energies correspond to the solutions of $\det\tilde{\Lambda}(0)=0$, $\det\tilde{\Lambda}(\theta)=0$, and $\det\tilde{\Lambda}(-\theta)=0$. After some straightforward algebraic manipulations we write the bulk spin-wave energies as $E_1(\mathbf{k})=\omega_{\mathbf{k}}(0)$, $E_2(\mathbf{k})=\omega_{\mathbf{k}}(\theta)$, and $E_3(\mathbf{k})=\omega_{\mathbf{k}}(-\theta)$, where

$$\omega_{\mathbf{k}}(\phi)=\pm\sqrt{[\Omega+\beta\exp(i\phi)+\beta^{*}\exp(-i\phi)]^2-[\alpha+\gamma\exp(i\phi)+\gamma^{*}\exp(-i\phi)]^2}. \tag{9}$$

In the appropriate limits, the spin-wave energies reduce to previously obtained results.[17,18] In Fig. 2 we plot the dispersion relations $E_1(\mathbf{k})$, $E_2(\mathbf{k})$, and $E_3(\mathbf{k})$ in the reduced and extended zone schemes. It is worth noting that the single mode $E_1(\mathbf{k})$ in an extended scheme will be equivalent to the three modes in a reduced scheme. The energy gap at the zone center for modes $E_2(\mathbf{k})$ and $E_3(\mathbf{k})$ [or equivalently for $E_1(4\pi/3,0,0)$] vanishes as $D\to 0$.

III. SEMI-INFINITE STACKED TRIANGULAR ANTIFERROMAGNET

In this section the properties of surface spin waves in a semi-infinite stacked triangular antiferromagnet are examined. The system considered has a (001) surface and is illustrated schematically in Fig. 3. Following the general approach used in previous works on semi-infinite systems,[9,11] the layers are labeled using a positive index $n(=1,2,3,\ldots)$, where the surface layer corresponds to $n=1$. The intralayer exchange and single-ion anisotropy parameters at the surface are allowed to differ from their respective bulk values. The intralayer exchange $J_{i,j}$ has the bulk value J everywhere except when both spins are on the surface layer where it has the value J_1. Likewise, the magnitude of the anisotropy for spins on interior bulk layers $(n>1)$ is written as D whereas for spins occupying sites at the surface it is D_1.

The spin-wave dispersion relations are obtained by forming the equations of motion for the operators $S_i^{\pm}$ $(i=l,m,n)$, where i is a site within the semi-infinite medium. The equations of motion for sites on the surface layer $(n=1)$ are different from those for interior bulk layers because sites at the surface interact with fewer interlayer neighbors and also because of the modified exchange and anisotropy parameters. In accordance with Bloch's theorem and the translational symmetry of the system in the xy plane, the equations of motion for the various spin deviation operators are transformed to a representation involving a two-dimensional wave vector $\mathbf{k}_{\parallel}=(k_x,k_y)$ which runs parallel to the surface and a layer index n. For example, for the lth site on sublattice A the wavelike solution for the spin operator is written as

$$S_l^{\pm}=S_{A,n}^{\pm}(\mathbf{k}_{\parallel})\exp[i(\mathbf{k}_{\parallel}\cdot\rho-Et)], \tag{10}$$

where $\boldsymbol{\rho}=(x,y)$ and the amplitudes $S_{A,n}^{\pm}(\mathbf{k}_{\parallel})$ depend on the z coordinate through the layer index n. Similar expressions are defined for sites on sublattices B and C. The compact notation $S_{A,n}^{\pm}(\mathbf{k}_{\parallel})\equiv S_{A,n}^{\pm}$ is used below. The system of finite difference equations connecting the Fourier amplitudes may be expressed in supermatrix form as $\mathbf{Mb}=0$, where $\mathbf{M}$ is an $\infty\times\infty$ block tridiagonal matrix defined as

$$\mathbf{M}=\begin{pmatrix}\mathbf{A}_1 & \boldsymbol{\tau} & 0 & 0 & 0 & \cdots\\ \boldsymbol{\tau} & \mathbf{A} & \boldsymbol{\tau} & 0 & 0 & \cdots\\ 0 & \tau & \mathbf{A} & \tau & 0 & \cdots\\ \vdots & \ddots & \ddots & \ddots & \ddots & \cdots\end{pmatrix} \tag{11}$$

and each element represents a 6×6 matrix. The matrix elements of $\mathbf{A}$ are defined as in Eqs. (4)–(7) except now $\Omega=2S\cos\theta J(0)-pSD-SJ'(0)$ and $\alpha=pSD$. The matrix $\mathbf{A}_1$ has the same form as $\mathbf{A}$ except the elements are defined by

$$\Omega_1=2S\cos\theta J_1(0)-pSD_1-SJ'(0)/2,$$

$$\alpha_1=pSD_1,$$

$$\beta_1=-S(1/2+\sigma)J_1(\mathbf{k}_{\parallel})/2,$$

$$\gamma_1=S(3/2+\sigma)J_1(\mathbf{k}_{\parallel})/2. \tag{12}$$

Also, the exchange dispersion $J_1(\mathbf{k}_{\parallel})$ is defined as in Eq. (7) but with $J\to J_1$. The 6×6 matrix $\boldsymbol{\tau}$ is a block diagonal matrix with each block given by

$$\tilde{\tau}=\frac{SJ'(0)}{4}\begin{pmatrix}2+\sigma' & -\sigma'\\ \sigma' & -2-\sigma'\end{pmatrix}. \tag{13}$$

The infinite column vector $\mathbf{b}$ is defined as $\mathbf{b}=[\mathbf{b}_1,\mathbf{b}_2,\ldots]^T$ with $\mathbf{b}_n=[S_{A,n}^{+},S_{A,n}^{-},S_{B,n}^{+},S_{B,n}^{-},S_{C,n}^{+},S_{C,n}^{-}]^T$. As in the bulk case, the equations may be partially decoupled by applying the transformation $\mathbf{U}^{\dagger}\mathbf{M}_{i,j}\mathbf{U}$ to all the elements of $\mathbf{M}$. This results into three linearly independent sets of equations which may be written in matrix form as $(\boldsymbol{\Lambda}_{\phi}+\Delta_{\phi})\mathbf{X}_{\phi}=0$ (for $\phi=0,\pm\theta$) where

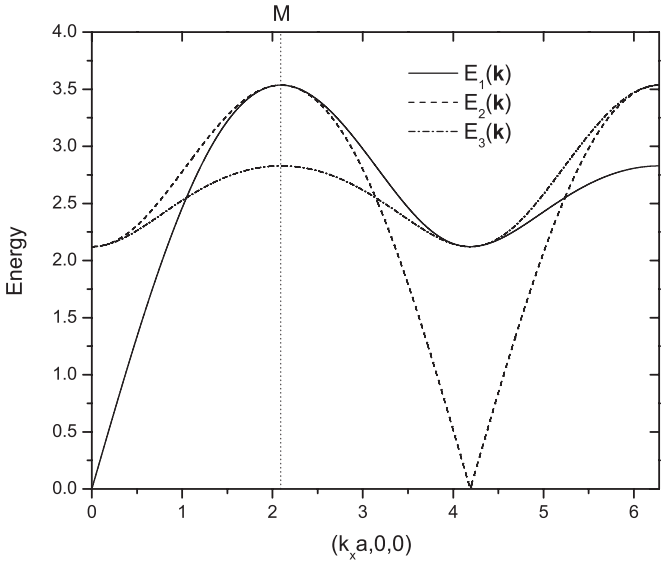

FIG. 2. The bulk spin-waves energies (in units of SJ) vs wave vector $(k_x a,0,0)$. The results are obtained using $J'=D=J$ with $\sigma=\sigma'=0$. The three modes $E_1(\mathbf{k})$, $E_2(\mathbf{k})$, and $E_3(\mathbf{k})$ are shown in a reduced and extended zone scheme. The M-point corresponds to the wave vector $\mathbf{k}=(2\pi/3,0,0)$.

$$\mathbf{\Lambda}_\phi = \begin{pmatrix} \tilde{\tau}^{-1}\tilde{\Lambda}(\phi) & \mathbb{1} & 0 & 0 & 0 & \cdots \\ \mathbb{1} & \tilde{\tau}^{-1}\tilde{\Lambda}(\phi) & \mathbb{1} & 0 & 0 & \cdots \\ 0 & \mathbb{1} & \tilde{\tau}^{-1}\tilde{\Lambda}(\phi) & \mathbb{1} & 0 & \cdots \\ \vdots & \ddots & \ddots & \ddots & \ddots & \cdots \end{pmatrix}. \tag{14}$$

The perturbation matrix Δ_ϕ has a single nonvanishing 2×2 element defined as

$$(\Delta_\phi)_{m,m'} = \tilde{\tau}^{-1}(\tilde{\Lambda}_1(\phi) - \tilde{\Lambda}(\phi))\,\delta_{m,1}\delta_{m',1}, \tag{15}$$

where $\tilde{\Lambda}_1(\phi)$ is defined as

$$\tilde{\Lambda}_1(\phi) = \tilde{A}_1 + \tilde{B}_1 \exp(i\phi) + \tilde{B}_1^* \exp(-i\phi)$$

and the column vector is

$$\mathbf{X}_\phi = [X_1^+(\phi), X_1^-(\phi), X_2^+(\phi), X_2^-(\phi), \ldots]^T$$

with elements

$$X_n^\pm(\phi) = \frac{1}{\sqrt{3}}(S_{A,n}^\pm + S_{B,n}^\pm \exp(-i\phi) + S_{C,n}^\pm \exp(i\phi)). \tag{16}$$

Following the approach used in other surface studies,[9,11] the matrix $(\Lambda_\phi+\Delta_\phi)$ may be written as $\mathbf{\Lambda}_\phi(\mathbf{I}+\mathbf{G}_\phi\Delta_\phi)$, where $\mathbf{I}$ is the unit supermatrix and $\mathbf{G}_\phi=\Lambda_\phi^{-1}$. This decomposition is particularly useful because the elements of $\mathbf{G}_\phi$ may be obtained analytically. The surface spin-wave modes correspond to the solutions of the determinantal condition

$$\det(\mathbf{I}+\mathbf{G}_\phi\Delta_\phi) = 0. \tag{17}$$

The elements of $\mathbf{G}_\phi$ are constructed following the approach used for simple cubic antiferromagnets.[11] The matrix

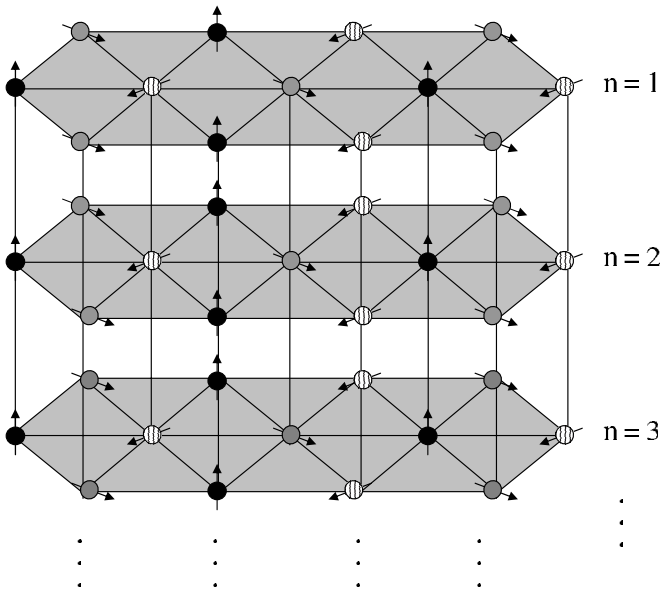

FIG. 3. Schematic view of a stacked triangular antiferromagnetic with a (001) crystallographic surface.

$\tilde{\tau}^{-1}\tilde{\Lambda}(\phi)$ is first diagonalized using the transformation $\tilde{V}^{-1}(\tilde{\tau}^{-1}\tilde{\Lambda}(\phi))\tilde{V}=\mathrm{diag}[\lambda_1,\lambda_2]$. The elements of the supermatrix $\mathbf{G}_\phi$ may be written as

$$(\mathbf{G}_\phi)_{m,m'} = -\tilde{V}\begin{pmatrix} f_{m,m'}(x_1) & 0 \\ 0 & f_{m,m'}(x_2) \end{pmatrix}\tilde{V}^{-1} \tag{18}$$

where

$$f_{m,m'}(x_i) = \frac{x_i^{m+m'} - x_i^{|m-m'|}}{x_i - x_i^{-1}}. \tag{19}$$

The complex quantities x_1 and x_2 are defined as

$$-(x_i + x_i^{-1}) = \lambda_i \text{ with } i = 1,2 \tag{20}$$

and satisfy $|x_1|\leqslant 1$ and $|x_2|\leqslant 1$. Because of the simple form of the perturbation matrix Δ_ϕ, Eq. (17) reduces to the determinant of a 2×2 matrix. Substituting Eq. (15) and (18) into Eq. (17), the determinantal condition becomes

$$\left| I - \tilde{V}\begin{pmatrix} x_1 & 0 \\ 0 & x_2 \end{pmatrix}\tilde{V}^{-1}\tilde{\tau}^{-1}(\tilde{\Lambda}_1(\phi) - \tilde{\Lambda}(\phi)) \right| = 0. \tag{21}$$

The surface spin-wave modes are obtained by solving Eq. (21) along with the requirement that $|x_1|<1$ and $|x_2|<1$. The bulk spin-waves correspond to $|x_1|=|x_2|=1$. Substituting $x_1=\exp(ik_z c)$ [or $x_2=\exp(ik_z c)$] in Eq. (20), where k_z is the third wave-vector component, the bulk dispersion relation in Eq. (9) may be obtained by solving for E. As in the bulk case (see Fig. 2), the spin-wave modes corresponding to the solutions of Eq. (21) with $\phi=\pm\theta$ can be obtained from those with $\phi=0$ by extending the range of wave vectors.

Figures 4 and 5 show the surface and bulk spin-wave dispersion relations in the $S=1$ semi-infinite triangular antiferromagnet vs $|\mathbf{k}_\parallel a|$. Here, the single-ion anisotropy at the surface is equal to the bulk value. In Fig. 4 the propagation

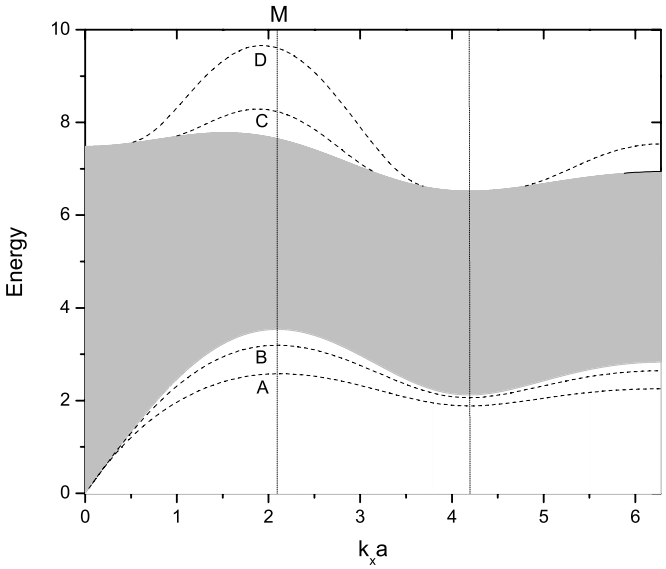

FIG. 4. Spin-wave energy (in units of SJ) in a semi-infinite $S=1$ frustrated antiferromagnet vs in-plane wave vector $k_x a$. We set $J'=D_1=D=J$ with $\sigma=\sigma'=0$ and show results for different values of intralayer exchange at the surface. The shaded area corresponds to the bulk continuum whereas the dashed curves labeled A, B, C, and D correspond to $J_1/J=0.5$, 0.75, 2.0, and 2.5, respectively. The M-point corresponds to the zone-edge wave vector $\mathbf{k}_\parallel=(2\pi/3,0)$.

wave vector is taken along the [100] direction whereas in Fig. 5 the wave vector is along the [010] direction. The dashed lines correspond to localized surface modes for different assumed values of the intralayer exchange J_1 at the surface. The bulk spin waves appear as an effective continuum in these plots with the upper and lower edges corresponding to $k_z c=\pi$ and $k_z c=0$, respectively. All of the modes are degenerate in magnitude and only the positive-frequency

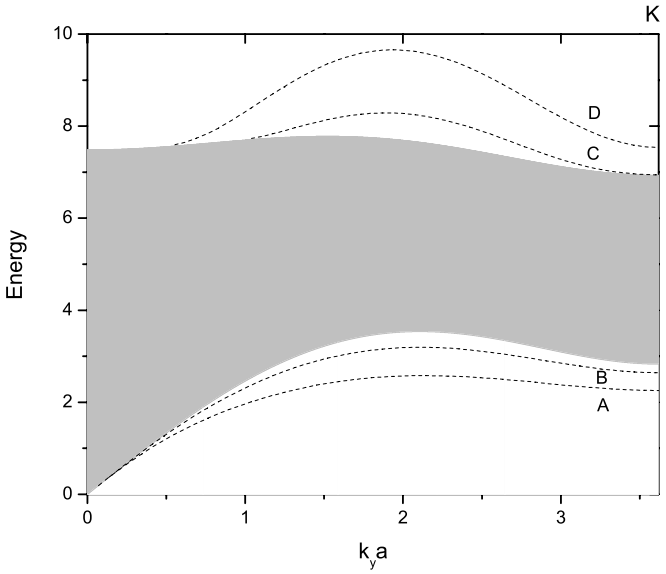

FIG. 5. Same as Fig. 4 but with in-plane wave vector taken along the y direction. The K-point corresponds to the zone-edge wave vector $\mathbf{k}_\parallel=(0,2\pi/\sqrt{3})$. The parameters used are the same as in Fig. 4.

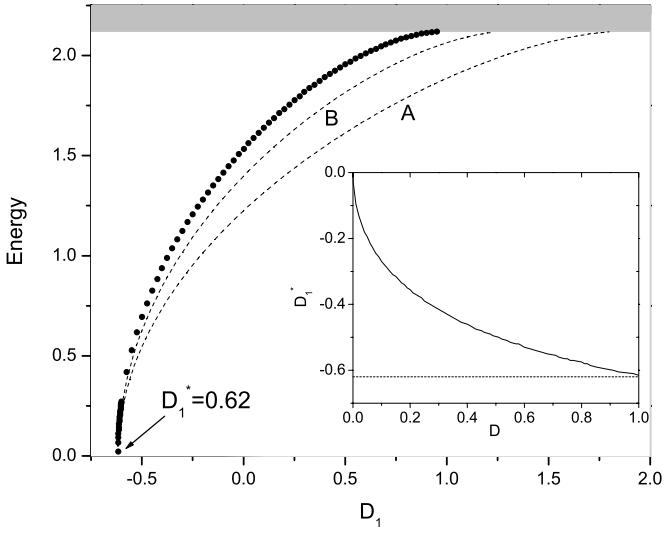

FIG. 6. Energy of the surface mode (in units of SJ) at wave vector $\mathbf{k}_\parallel=(4\pi/3,0)$ as a function of surface anisotropy D_1. All of the curves are obtained using $J'=D=J=1.0$ with $\sigma=\sigma'=0$ and results are shown for different values of exchange J_1. The curves labeled A and B are as in Fig. 4 with $J_1=0.5$ and 0.75, respectively, whereas the filled circles correspond to $J_1=J$. The energy gap vanishes for $D_1^*\approx-0.62$. The inset shows the dependence of the critical value of the surface anisotropy D_1^* as a function of the bulk anisotropy D.

solutions are shown. The case with $J_1=J$ (not shown) corresponds to a surface branch that appears just below the lower edge of the bulk region. The surface branches with $J_1>J$ (curves C and D) are truncated modes and only exist at certain values of the wave vector $\mathbf{k}_\parallel$. As in unfrustrated magnetic systems, the surface branches are found to be extremely sensitive to the values of exchange and anisotropy parameters at the surface. The surface branches located near the bulk continuum regions are deeply penetrating modes. In contrast, surface modes that are far from the continuum regions are more localized near the surface. The gapless spin-wave excitation at $\mathbf{k}_\parallel=0$ corresponds to the Goldstone mode. This uniform mode reflects the fact that there is no cost in energy in rotating the spin configuration depicted in Fig. 3 about the c axis.

The effect of the single-ion anisotropy on the surface spin-wave energy is depicted in Fig. 6. The graph shows the energy of the surface mode at $\mathbf{k}_\parallel=(4\pi/3,0)$ as a function of the surface anisotropy D_1 for different values of intralayer exchange J_1. The bulk exchange and anisotropy parameters are $J'=D=J=1.0$ (with $\sigma=\sigma'=0$) and the shaded area represents the lower edge of the bulk continuum. The energy gap of the surface mode remains finite when $D_1=0$ (for $D>0$ and $J'>0$) because of the coupling between the spins in the surface layer and the interior bulk layers. The effects of the bulk anisotropy D on the surface spin-wave modes at $\mathbf{k}_\parallel=(4\pi/3,0)$ are canceled at the critical value $D_1^*\approx-0.62$ and the system is effectively isotropic for these modes. Below the critical value the ground state configuration with the spins in the surface layers lying in the xy plane (as depicted schematically in Fig. 3) becomes unstable. This is analogous to the surface reorientation phase transition predicted in

other anisotropic magnetic systems.[26] The critical value of the surface anisotropy D_1 is found to be independent of the surface exchange J_1 (as shown in Fig. 6) but depends strongly on the values of the bulk anisotropy D. The inset in Fig. 6 shows the critical surface anisotropy vs the bulk anisotropy for the case of $J'=J=1.0$. In the absence of bulk anisotropy ($D=0$) the critical value of the surface anisotropy is $D_1^*=0$, as expected.

IV. STACKED TRIANGULAR ANTIFERROMAGNETIC THIN FILM

The properties of surface and bulk spin waves in stacked triangular antiferromagnetic thin films may be investigated by extending the results of the previous section. For a film composed of N layers the system of finite difference equations may again be expressed in supermatrix form as $\mathbf{Mb}=0$ where $\mathbf{M}$ is now a $6N\times 6N$ block-tridiagonal matrix. As in the semi-infinite case the surface parameters for the antiferromagnetic exchange and single-ion anisotropy are allowed to differ from the bulk values. For layer $n=N$, the intralayer exchange is written as J_N and the anisotropy as D_N.

Following an approach similar to that described in Sec. III the transformation $\mathbf{U}^+\mathbf{M}_{i,j}\mathbf{U}$ is first applied to the elements of $\mathbf{M}$. The resulting set of equations may be expressed as three linearly independent matrix equations as $(\mathbf{\Lambda}_\phi+\Delta_\phi)\mathbf{X}_\phi=0$ (for $\phi=0,\pm\theta$) where $\mathbf{\Lambda}_\phi$ is now a $2N\times 2N$ matrix with elements defined as in Eq. (14) and the column vector is $\mathbf{X}_\phi=[X_1^+(\phi),X_1^-(\phi),\ldots,X_N^+(\phi),X_N^-(\phi)]^T$. The matrix Δ_ϕ describing the perturbation due to the surfaces of the thin film has two nonvanishing 2×2 blocks at the ends of the leading diagonal and may be written as

$$(\Delta_\phi)_{m,m'}=\tilde{\tau}^{-1}(\tilde{\Lambda}_\mu(\phi)-\tilde{\Lambda}(\phi))\,\delta_{m,\mu}\delta_{m',\mu},\quad \mu=1,N, \tag{22}$$

where $\tilde{\Lambda}_N(\phi)=\tilde{A}_N+\tilde{B}_N\exp(\phi)+\tilde{B}_N^*\exp(-i\phi)$. The matrix elements of $\tilde{A}_N$ ($\tilde{B}_N$) are defined as in Eq. (12) but with the modified exchange and anisotropy parameters at the surface layer $n=N$. The elements of $\mathbf{G}_\phi$ may be written as in Eq. (18) but now with

$$f_{m,m'}(x_i)=\frac{x_i^{m+m'}-x_i^{|m-m'|}+x_i^{2N+2-(m+m')}-x_i^{2N+2-|m-m'|}}{(1-x_i^{2N+2})(x_i-x_i^{-1})}. \tag{23}$$

The complex parameters x_i ($i=1,2$) are defined as in Eq. (20) and satisfy $|x_i|\leq 1$. The solution of Eq. (17) for a film composed of N layers reduces to solving the 4×4 determinantal condition

$$\det(\mathbf{I}+\mathbf{G}_\phi\Delta_\phi)=\begin{vmatrix} I+(\mathbf{G}_\phi)_{1,1}(\Delta_\phi)_{1,1} & (\mathbf{G}_\phi)_{1,N}(\Delta_\phi)_{N,N} \\ (\mathbf{G}_\phi)_{1,N}(\Delta_\phi)_{1,1} & I+(\mathbf{G}_\phi)_{1,1}(\Delta_\phi)_{N,N}\end{vmatrix}=0. \tag{24}$$

The solutions of Eq. (24) will consist of surface modes corresponding to $|x_i|<1$ and a set of quantized bulk modes with $|x_i|=1$ ($i=1,2$). In the limit of $N\to\infty$ the elements of the matrix $(\mathbf{G}_\phi)_{1,N}$ vanish and the determinantal condition (24) reduces to $\det(I+(\mathbf{G}_\phi)_{1,1}(\Delta_\phi)_{1,1})=0$ and $\det(I+(\mathbf{G}_\phi)_{1,1}(\Delta_\phi)_{N,N})=0$. In the case of symmetric surfaces ($J_1=J_N$ and $D_1=D_N$) both determinantal conditions reduce to Eq. (21) for the semi-infinite system and the surface modes are degenerate, as expected. Also, it is easily verified that the determinantal condition is invariant with respect to the interchange of exchange and anisotropy parameters at the surfaces ($J_1\Leftrightarrow J_N$ and $D_1\Leftrightarrow D_N$).

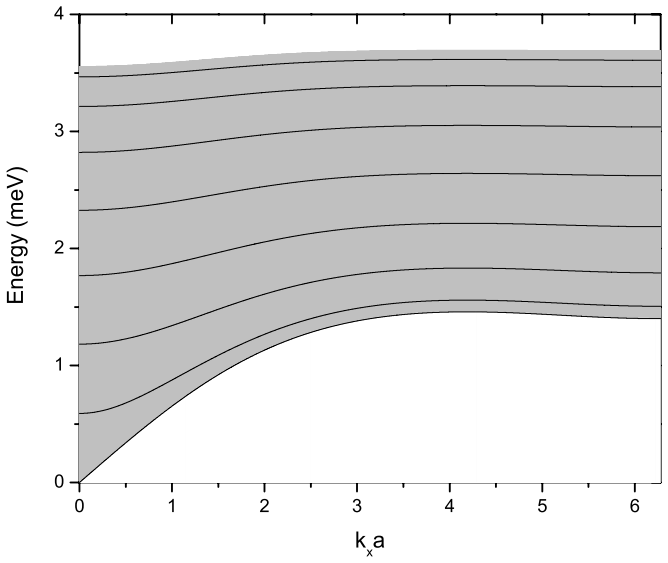

FIG. 7. Spin-wave energy vs k_xa for $RbFeCl_3$. The physical parameters are given in the main text. The solid lines represent the spin-wave branches for a thin film composed of $N=8$ layers and the shaded area corresponds to the effective bulk continuum.

Figure 7 shows numerical results for the $S=1$ quasi-1D hexagonal compound $RbFeCl_3$ with ferromagnetic interplane and antiferromagnetic intraplane exchange which exhibits the 120° in-plane structure at $T<1.95$ K.[27,28] The approximate values of the exchange and anisotropy parameters are known from inelastic neutron scattering: $J=0.068$ meV, $J'=0.488$ meV, $\sigma=\sigma'=-0.06$, and $D=1.7$ meV. The exchange and anisotropy parameters are assumed uniform throughout the thickness of the material. For these parameter values there is a single surface mode located just below the effective bulk continuum. The splitting of the surface branch from the bulk region can be enhanced with a small perturbation of the surface parameters. The quasi-one-dimensionality of $RbFeCl_3$ results in bulk spin-waves having a weak dependence on the in-plane wave vector $\mathbf{k}_\parallel$.

In Fig. 8 the spin-wave modes for a thin film of $RbFeCl_3$ composed of $N=5$ layers are shown. The solid lines show results for a symmetric film with $D_1=D_N=0.5D$ and $J_1=J_N=J$. For these parameter values the surface modes are below the effective bulk region. The dashed lines show the spin-wave energies for the case of asymmetric surface anisotropy parameters. Here, $D_1=0.25D$, $D_N=0.5D$ and the intralayer exchange is taken to be uniform throughout the thickness of the film. The single-ion anisotropy is a site dependent quantity that depends on the local crystalline electric field which may be different near the surfaces of the film compared with

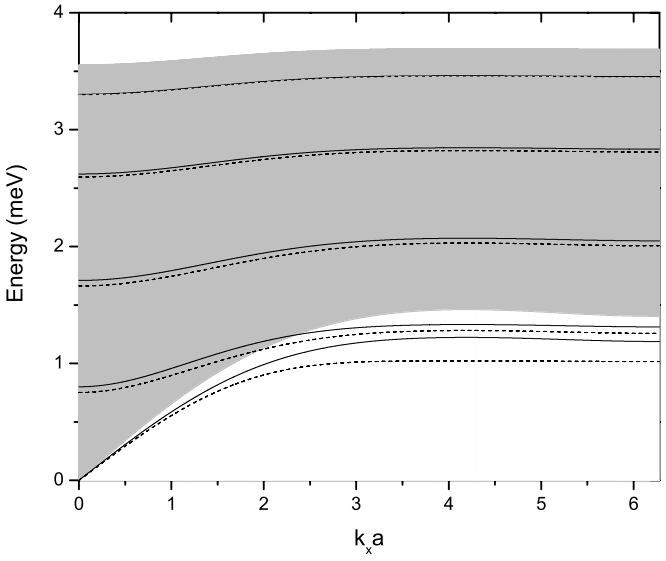

FIG. 8. Spin-wave energy vs in-plane wave vector $k_x a$ for a thin film of $RbFeCl_3$ with $N=5$ layers. The solid lines correspond to $D_1=D_N=0.5D$ and for the dashed lines $D_1=0.25D$, $D_N=0.5D$. For both sets of curves the exchange parameters are $J_1=J_N=J$.

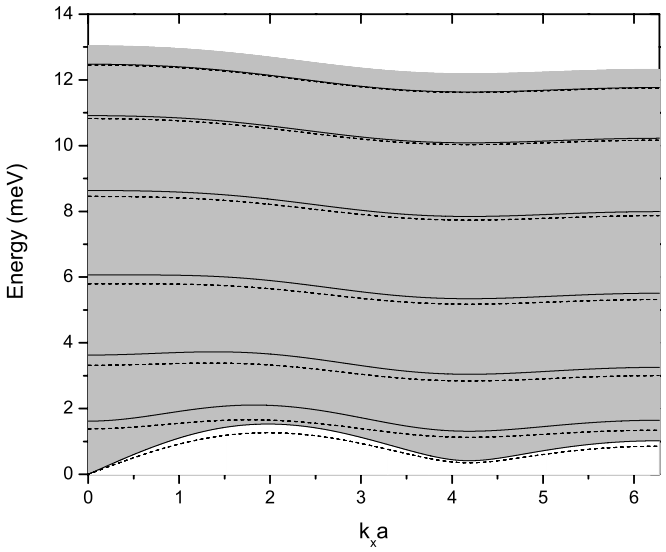

FIG. 9. Spin-wave energy vs in-plane wave vector $k_x a$ (with $k_y=0$) for a thin film of $CsCuCl_3$ with $N=7$ layers. The solid lines correspond to surface exchange parameters $J_1=J_N=J$ and the dashed lines are the results with $J_1=J_N=0.5J$.

the bulk. Magnetic films sandwiched between different nonmagnetic layers can create surface asymmetry. The asymmetry in the film enhances the splitting between the surface modes at larger wave vectors.

Another hexagonal system characterized with a strong ferromagnetic interlayer exchange and weak intralayer exchange is the $S=1/2$ compound $CsCuCl_3$.[15] A model similar to the one used here has been previously employed to investigate the properties of spin waves in bulk $CsCuCl_3$ (Ref. 29) and the estimated parameter values are $J=1.0$ meV; $J'=5.5$ meV; $\sigma=-0.054$, $\sigma'=0.0$. A weak Dzyaloshinsky-Moriya interaction which is believed to be responsible for the rotation of the triangular spin configuration between successive planes in $CsCuCl_3$ is neglected here. The terms in the equations of motion involving the single-ion anisotropy [see Eqs. (6) and (12)] will vanish for $CsCuCl_3$ because $p=0$ for $S=1/2$ systems. Numerical results for the spin-wave dispersion in a thin film of $CsCuCl_3$ composed of 7 layers are shown in Fig. 9. The solid lines represents the results using uniform values of the exchange interaction throughout the thickness of the film whereas the dashed lines are the results using $J_1=J_N=0.5J$. The gap in the spectrum at $\mathbf{k}_\parallel=(4\pi/3,0)$ is due to the anisotropic exchange parameter σ. The quasi-1D character of the system is evident from the weak dependence of the spin-wave energies on the in-plane wave vector. As in the previous cases the splitting between the surface modes and the effective bulk region may be enhanced by allowing for modified values of the exchange coupling in the surface layer.

V. CONCLUSIONS

A method to obtain magnetic dispersion relations for surface and bulk spin waves in the stacked triangular antiferromagnet has been presented. The theory was developed for a semi-infinite system and generalized to the case of a thin film composed of a finite number of layers. The decoupling approximations used to linearized the equations of motion are valid in the low-temperature limit $T \ll T_N$, and therefore the results are confined to this temperature regime. The calculations were carried out explicitly for the case of ferromagnetic coupling between interlayer nearest neighbors and the theory was applied to $RbFeCl_3$ and $CsCuCl_3$. The influence of modified exchange and anisotropy parameters at the surface(s) was investigated and it was found that surface spin waves can be well- separated in frequency from bulk spin waves with small differences between the surface parameters compared to the bulk values. At the present time we are not aware of any experimental studies concerning the magnetic properties of atoms located near the surface of frustrated magnetic materials. Appropriate experimental techniques to test the theoretical predictions described in this paper may include spin-polarized particles (such as SPEELS) and spin-wave resonance.[6,30] Inelastic light scattering may also be suitable to investigate the spin-wave modes near the zone center.

The formalism used here may be extended to investigate the spin-wave properties for the case of antiferromagnetic coupling between layers and applications can be made to a wide variety of frustrated triangular antiferromagnets.[15] For such systems, a six sublattice model may be employed and for the bulk spin waves 12 equations of motion are required to obtain a closed set. For thin films with antiferromagnetic interlayer coupling and (001) surfaces, the surface spin-wave modes are expected to show distinct features depending on whether the total number of layers is even or odd. The effect of the inequivalence between sublattices on the characteristics of surface spin waves has been investigated in simple cubic antiferromagnetic films with (111) surfaces[13] and metamagnetic thin films.[25]

From the theoretical standpoint there are various other possible extensions of this work. It it well-known that the

characteristic properties of surface spin waves in ferromagnets and antiferromagnets depend strongly on the surface orientation. In frustrated materials the effect of surface orientation on the properties of surface spin waves may be even greater because of the quasi- one- and two-dimensionality observed in these systems. Another possible extension would be to carry out Green function calculations to extract the spin-spin correlations functions. This typically involves solving inhomogeneous matrix equations[9] as opposed to the operator equation of motion technique employed here which requires solving homogeneous equations. The correlation functions can be used to determine the dynamic magnetic response for a variety of frustrated magnetic materials and compared to experimental results. Future applications of these approaches will include thin films of stacked triangular magnetoelectric $RMnO_3$ compounds.[31,32]

ACKNOWLEDGMENTS

This work was partially supported by the Natural Sciences and Engineering Research Council of Canada (NSERC).

*Electronic address: eric@physics.mun.ca

[1] H. Ohldag, A. Scholl, F. Nolting, S. Anders, F. U. Hillebrecht, and J. Stöhr, Phys. Rev. Lett. **86**, 2878 (2001).
[2] F. U. Hillebrecht, H. Ohldag, N. B. Weber, C. Bethke, U. Mick, M. Weiss, and J. Bahrdt, Phys. Rev. Lett. **86**, 3419 (2001).
[3] D. L. Mills, in *Surface Excitations*, edited by V. M. Agranovich and R. Loudon (North-Holland, Amsterdam, 1984), p. 379.
[4] M. G. Cottam and D. R. Tilley, *Introduction to Surface and Superlattice Excitations*, 2nd ed. (IOP Publishing, Bristol, 2004).
[5] M. Plihal, D. L. Mills, and J. Kirschner, Phys. Rev. Lett. **82**, 2579 (1999).
[6] R. Vollmer, M. Etzkorn, P. S. Anil Kumar, H. Ibach, and J. Kirschner, Phys. Rev. Lett. **91**, 147201 (2003).
[7] T. Wolfram and R. E. DeWames, Prog. Surf. Sci. **2**, 233 (1972).
[8] D. L. Mills and W. M. Saslow, Phys. Rev. **171**, 488 (1968).
[9] M. G. Cottam, J. Phys. C **9**, 2121 (1976).
[10] S. Gopalan and M. G. Cottam, Phys. Rev. B **42**, 624 (1990).
[11] T. Wolfram and R. E. DeWames, Phys. Rev. **185**, 762 (1969).
[12] M. G. Cottam and D. Kontos, J. Phys. C **13**, 2945 (1980).
[13] J. M. Pereira, Jr. and M. G. Cottam, Phys. Rev. B **63**, 174431 (2001).
[14] V. Thanh Ngo and H. T. Diep, cond-mat/0409543 (to be published).
[15] M. F. Collins and O. A. Petrenko, Can. J. Phys. **75**, 605 (1997).
[16] *Magnetic Systems with Competing Interactions*, edited by H. T. Diep (World Scientific, Singapore, 1994).
[17] T. Oguchi, J. Phys. Soc. Jpn. **52**, 183 (1983).
[18] O. P. Vajk, M. Kenzelmann, J. W. Lynn, S. B. Kim, and S. W. Cheong, Phys. Rev. Lett. **94**, 087601 (2005).
[19] B. D. Gaulin, M. F. Collins, and W. J. L. Buyers, J. Appl. Phys. **61**, 3409 (1987).
[20] O. A. Petrenko, M. F. Collins, C. V. Stager, and Z. Tun, Phys. Rev. B **51**, 9015 (1995).
[21] J. A. Oyedele and M. F. Collins, Can. J. Phys. **56**, 1482 (1978).
[22] R. M. Morra, W. J. L. Buyers, R. L. Armstrong, and K. Hirakawa, Phys. Rev. B **38**, 543 (1988).
[23] A. B. Harris, C. Kallin, and A. J. Berlinsky, Phys. Rev. B **45**, 2899 (1992).
[24] K. Sugawara and I. Yamada, J. Phys.: Condens. Matter **5**, 1427 (1993).
[25] E. Meloche and M. G. Cottam, Phys. Rev. B **70**, 094423 (2004).
[26] D. L. Mills, in *Ultrathin Magnetic Structures I*, edited by J. A. C. Bland and B. Heinrich (Springer, Berlin, 1994), p. 91.
[27] H. Yoshizawa, W. Kozukue, and K. Hirakawa, J. Phys. Soc. Jpn. **49**, 144 (1980).
[28] G. R. Davidson, M. Eibscutz, D. E. Cox, and V. J. Minkiewitz, in *Magnetism and Magnetic Materials-1991*, edited by C. D. Graham and J. J. Rhyne, AIP Conf. Proc. No. 5 (AIP, New York, 1972), p. 436.
[29] E. Rastelli and A. Tassi, Phys. Rev. B **49**, 9679 (1994).
[30] S. F. Alvarado, E. Kisker, and M. Campagna, in *Magnetic Properties of Low-Dimensional Systems*, edited by L. M. Falicov and J. L. Moran-Lopez (Springer, Heidelberg, 1986).
[31] J. Dho and M. G. Blamire, Appl. Phys. Lett. **87**, 252504 (2005).
[32] X. Martí, F. Sánchez, J. Fontcuberta, M. V. Garcia-Cuenca, C. Ferrater, and M. Varela, J. Appl. Phys. **99**, 08P302 (2006).